Femtosecond Solvation Dynamics in a Micron-Sized Aggregate of an Ionic Liquid and P123 Triblock Copolymer

Shantanu Dey, Aniruddha Adhikari, Dibyendu Kumar Das, Dibyendu Kumar Sasmal, and Kankan Bhattacharyya*

Department of Physical Chemistry, Indian Association for the Cultivation of Science, Jadavpur, Kolkata 700 032, India

Received: May 19, 2008; Revised Manuscript Received: October 5, 2008

Dynamic light scattering studies indicate that addition of a room temperature ionic liquid (RTIL, [pmim][Br]), to a triblock copolymer (P123) micelle leads to the formation of giant P123-RTIL clusters of size (diameter) 40 nm in 0.9 M and 3500 nm (3.5 μm) in 3 M RTIL. They are much larger than a P123 micelle (~18 nm) or [pmim][Br] (1.3 nm). Dynamics in different regions of the P123-RTIL aggregate is probed by variation of the excitation wavelength (λ_{ex}) using femtosecond up-conversion. For $\lambda_{ex} = 375$ nm, the nonpolar core of the P123-RTIL aggregate is preferentially excited while $\lambda_{ex} = 435$ nm selects the polar corona region. Solvation dynamics and anisotropy decay of coumarin 480 (C480) in a P123-RTIL giant aggregate are markedly different from those in either P123 micelle or those in an aqueous solution of the RTIL. For $\lambda_{ex} = 405$ nm in 5 wt % P123 and 0.9 M RTIL average rotational time, ($<\tau_{rot}> = 1350$ ps) of C480 is ~7 times longer than that (200 ps) in an aqueous solution of the RTIL in the absence of P123 and is shorter than that (3000 ps) in a P123 micelle. In 0.9 M RTIL and 5 wt % P123, solvation dynamics in the corona region ($\lambda_{ex} = 435$ nm, $<\tau_s> =$ 75 ps) is ~25 times faster than that at the core region (at $\lambda_{ex} = 375$ nm, $<\tau_s> = 1900$ ps). The solvation dynamics in the core of the P123-RTIL aggregate is faster than that in P123 micelle (3550 ps in the core) and is much slower than that (130 ps) in an aqueous solution containing 0.9 M RTIL. In the 3.5 μm sized aggregate (3 M RTIL and P123), the solvation dynamics in the core ($<\tau_s> = 500$ ps) is ~4 times faster than that in 0.9 M RTIL.

1. Introduction

The room temperature ionic liquids (RTILs) have received vigorous recent attention as an environmentally benign ("green") solvent with tailor-made properties and as a catalyst for many organic reactions.[1,2] The low melting point (because of the steric hindrance) and the high boiling point (arising from interionic attractions) keep an RTIL in the liquid phase for a large temperature range. Many recent experiments[3−5] and simulations[6,7] addressed the structure, dynamics, and solvation properties of the RTILs. According to computer simulations, many RTILs display nanoscale structural organization with clear segregation of the polar (ions) and nonpolar (alkyl side chain) domains.[1a,7] Recent X-ray scattering,[8a] optical heterodyne Kerr spectroscopy,[8b] and Raman spectroscopic[9] investigations confirm presence of nanoaggregates of size 1.3−2.7 nm in RTILs for alkyl chains containing 4−10 carbon atoms. Most recently, excitation wavelength dependence of solvation dynamics demonstrated presence of dynamic heterogeneity in a neat RTIL.[4a,10a]

In the present work, we report on the interaction of a triblock copolymer, $(PEO)_{20}$-$(PPO)_{70}$-$(PEO)_{20}$ (Pluronic P123) with an ionic liquid, 1-pentyl-3-methyl-imidazolium bromide ([pmim][Br], Scheme 1A). The structure of a P123 micelle has been thoroughly investigated using small-angle neutron scattering (SANS), small-angle X-ray scattering (SAXS), and NMR.[11] According to SANS studies, a P123 micelle consists of a hydrophobic core (PPO block) with a radius of 4.8 nm and a hydrophilic corona (PEO block) of thickness 4.6 nm so that the overall diameter is ~18 nm (Scheme 1C).[11]

SCHEME 1: Schematic Representation of (A) [pmim][Br], (B) Coumarin 480 (C480), (C) P123 Micelle, and (D) P123-[pmim][Br] Aggregate

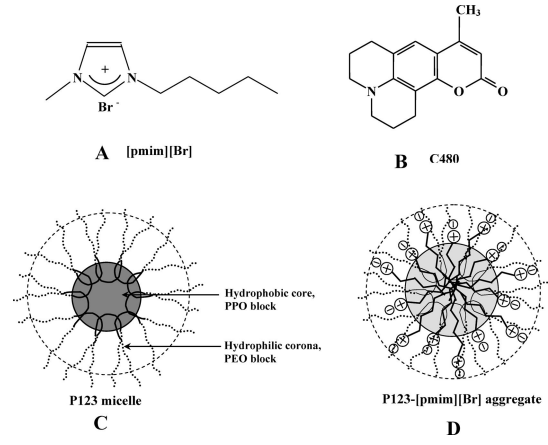

It may be tempting to understand the effect of an ionic liquid on a micelle in terms of salt effect on the stability of micellar and biological assemblies (the so-called Hofmeister effect[12]). According to the Hofmeister effect,[12] small ions decrease solubility of organic residues of a protein or a surfactant in water ("salting-out"). This increases the stability of the structure of a protein or a micelle and leads to the lowering of critical micellar concentration (CMC). However, the effect of the ionic liquid (RTIL) on a micelle is qualitatively different and more complicated than that of an ordinary salt (NaCl or NaSCN).[13] First, the effect of RTIL is nonmonotonic. CMC of sodium

* To whom correspondence should be addressed. E-mail: pckb@mahendra.iacs.res.in. Fax: (91)-33-2473-2805.

10.1021/jp804401p CCC: $40.75
Published on Web 01/05/2009

dodecyl sulfate (SDS), decreases on addition of a RTIL at a low concentration.[13c] But at a high concentration, the same RTIL causes an increase of CMC of SDS. [13c] In the case of triton X-100, though addition of RTIL does not have appreciable effect on the CMC the structure of the micelle is markedly modified on addition of RTIL.[13d] Zheng et al. showed that addition of an ionic liquid, 1-butyl-3-methyl-imidazolium bromide ([bmim-][Br]) affects aggregation of the triblock copolymer, $(PEO)_{27}$-$(PPO)_{61}$-$(PEO)_{27}$ (Pluronic P104) and at a high concentration of the RTIL (>1 M) very large aggregates with a diameter of ~500 nm (0.5 μm) are formed.[13a] In this work, using dynamic light scattering (DLS) we show that addition of the RTIL substantially modifies the structure of a P123 micelle, and the [pmim][Br]-P123 aggregate is much larger than the P123 micelle.

Finally, we have applied femtosecond up-conversion to study solvation dynamics and anisotropy decay in the [pmim][Br]-P123 aggregate. We have studied the dynamics in different regions of this aggregate (mixed micelle) by variation of the excitation wavelength (λ_{ex}). For this purpose we use a dye, coumarin 480 (C480), which is soluble in both polar (e.g., water, alcohol) and nonpolar (e.g., *n*-hexane) solvents and whose spectral properties depend on solvent polarity.[14] In a heterogeneous medium (e.g., a P123-RTIL mixed micelle), absorption and emission maxima of C480 vary markedly from one region to another. At a short λ_{ex}, the probe (C480) molecules in a relatively nonpolar environment (e.g., core of a P123 micelle) are preferentially excited giving rise to a blue-shifted emission spectrum. Excitation at a longer wavelength (red edge) selects the probe in a relatively polar environment (corona of a P123 micelle) and results in a red-shifted emission spectrum. The λ_{ex} dependence of emission maximum is known as red edge excitation shift (REES).[15] Recently, using λ_{ex} dependence we have studied solvation dynamics in different regions of neat RTIL,[10a] RTIL microemulsions,[10a] RTIL mixed micelle,[10b] a P123 micelle,[16] in a water containing microemulsion,[17a] a lipid vesicle,[17b,c] P123-SDS aggregate,[17d] P123 gel,[17e] and bile salt aggregate.[17f] In this work, we show that the solvation dynamics of C480 in a P123-RTIL aggregate is different from that in a P123 micelle and that in an aqueous solution of the RTIL.

2. Experimental Section

Laser grade coumarin 480 (C480, Exciton, Scheme 1B) was used as received. The triblock copolymer, Pluronic P123 (P123, Scheme 1C) was a gift from BASF Corp. and was used without further purification. 1-methylimidazole (99%, Aldrich) and 1-bromopentane (99%, Aldrich) were used for the synthesis of the RTIL. Acetonitrile (Merck) was distilled over P_2O_5 and dichloromethane (Merck) was used as received. Diethyl ether (Merck) was distilled over KOH.

The RTIL, [pmim][Br] (Scheme 1A), was prepared from 1-methylimidazole and 1-bromopentane following the sonochemical route.[18] For purification, the raw [pmim][Br] was diluted with dicholoromethane and filtered a couple of times through a silica gel column. The filtrate was treated with activated charcoal in an inert atmosphere for 48 h to remove any possible trace of color. After removal of dicholoromethane in a rotary evaporator, [pmim][Br] was repeatedly washed with dry diethyl ether to yield the RTIL in form of almost colorless, viscous liquid.

The copolymer solution was prepared by stirring the proper amount of the copolymer (P123) with 100 mL of water for 4−5 h at room temperature in a sealed container. We used 5 wt % P123 (~8.7 mM). This is much higher than the CMC of P123 (0.18 wt %, 0.30 mM). All experiments were done at room temperature (~20° C). The steady state absorption and emission spectra were recorded in a Shimadzu UV-2401 spectrophotometer and a Spex FluoroMax-3 spectrofluorimeter, respectively.

In our femtosecond upconversion setup (FOG 100, CDP) the sample was excited at 375, 405, and 435 nm using the second harmonic of a mode-locked Ti-sapphire laser (Tsunami, Spectra Physics), pumped by a 5 W Millennia (Spectra Physics). In order to generate second harmonic, we used a nonlinear crystal (1 mm BBO, $\theta = 25°$, $\phi = 90°$). The fluorescence emitted from the sample was upconverted in a nonlinear crystal (0.5 mm BBO, $\theta = 38°$, $\phi = 90°$) using the fundamental beam as a gate pulse. The upconverted light is dispersed in a monochromator and detected using photon counting electronics. A cross-correlation function obtained using the Raman scattering from ethanol displayed a full width at half-maximum (fwhm) of 350 fs. The femtosecond transients were fitted using a Gaussian shape for the exciting pulse.

The femtosecond transients are fitted keeping the long picosecond components fixed. To determine the picosecond components, the samples were excited at 375, 405, and 435 nm using picosecond diode lasers (IBH nanoleds) in an IBH Fluorocube apparatus. The emission was collected at a magic-angle polarization using a Hamamatsu MCP photomultiplier (5000U-09). The time-correlated single photon counting (TC-SPC) setup consists of an Ortec 9327 CFD and a Tennelec TC 863 TAC. The data is collected with a PCA3 card (Oxford) as a multichannel analyzer. The typical fwhm of the system response using a liquid scatterer is about 90 ps. The picosecond fluorescence decays were deconvoluted using IBH DAS6 software. All experiments were done at room temperature (293 K).

In order to study fluorescence anisotropy decay, the analyzer was rotated at regular intervals to get perpendicular ($I_\perp$) and parallel ($I_{||}$) components. Then the anisotropy function, $r(t)$ was calculated using the formula

$$r(t) = \frac{I_{||}(t) - GI_\perp(t)}{I_{||}(t) + 2GI_\perp(t)} \quad (1)$$

The G value of the picosecond setup was determined using a probe whose rotational relaxation is very fast, (e.g., C480 in methanol), and the G value was found to be 1.5.

The time-resolved emission spectra (TRES) were constructed using the parameters of best fit to the fluorescence decays and the steady state emission spectrum following the procedure described by Maroncelli and Fleming.[19a] The solvation dynamics is described by the decay of the solvent correlation function $C(t)$, defined as

$$C(t) = \frac{\nu(t) - \nu(\infty)}{\nu(0) - \nu(\infty)} \quad (2)$$

where $\nu(0)$, $\nu(t)$, and $\nu(\infty)$ are the emission maxima (frequencies) at time 0, t, and ∞, respectively. Note, a portion of solvation dynamics is missed even in our femtosecond setup of time resolution 350 fs. The amount of solvation missed is calculated using the Fee−Maroncelli procedure.[19b] The emission frequency at time zero, $\nu^p_{em}(0)$ may be calculated using the absorption frequency (ν^p_{abs}) in a polar medium (i.e., C480 in [pmim][Br]) as[19b]

$$\nu^p_{em}(0) = \nu^p_{abs} - (\nu^{np}_{abs} - \nu^{np}_{em}) \quad (3)$$

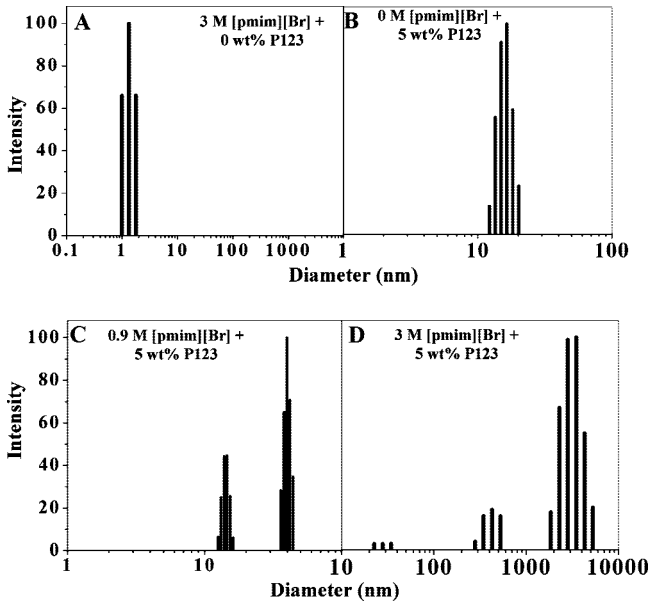

Figure 1. Size distribution of the droplets (measured by dynamic light scattering) in the presence of (A) 3 M [pmim][Br] in 0 wt % P123 and (B) 0 M, (C) 0.9 M, and (D) 3 M [pmim][Br] in 5 wt % P123.

TABLE 1: DLS Data on Diameters of 5 wt % P123 Micelle in the Presence of [pmim][Br]

concentration of RTIL (M) (χ_{IL})[a]	effective diameter[b] (nm)	polydispersity index
0 (0)	18	0.150
0.3 (0.006)	26	0.141
0.6 (0.012)	37	0.162
0.9 (0.019)	40	0.184
1.2 (0.026)	104	0.247
1.8 (0.044)	560	0.379
2.4 (0.066)	1725	0.451
3 (0.095)	3480	0.414

[a] Mole fraction of RTIL, $\chi_{IL} = (n_{IL})/(n_{IL} + n_{P123} + n_{Water})$. [b] Major component.

Where ν_{em}^{np} and ν_{abs}^{np} denote the steady-state frequencies of emission and absorption, respectively, of the probe (C480) in a nonpolar solvent (i.e., cyclohexane).

The effective diameter and polydispersity index were determined by DLS using a Brookhaven BI-200SM Goniometer (Brookhaven Instruments Corporation) with a 35 mW He−Ne laser (633 nm).

3. Results and Discussion

3.1. Dynamic Light Scattering Studies: Structure of P123-[pmim][Br] Aggregate. In this section, we report on the effect of [pmim][Br] on the structure (size) of the P123-RTIL. Our DLS study shows formation of a micron-sized aggregate containing P123 and the RTIL, [pmim][Br] which are much bigger than a P123 micelle. Interestingly, such a big particle is not detected in an aqueous solution of [pmim][Br] in the absence of P123. In the absence of P123, a 3 M aqueous solution of [pmim][Br] exhibits a single peak at ~1.3 nm and there is none in the range ~10−10 000 nm (Figure 1A and Table 1).

The diameter of a P123 micelle is ~18 nm (Table 1 and Figure 1B).[11] On addition of [pmim][Br], the contribution of the P123 micelles (~18 nm) decreases and a much larger particle is formed. In 0.9 M [pmim][Br] and 5 wt % P123, the major (~70%) contribution to the DLS signal arises from a particle of diameter 40 nm (Figure 1C) and ~30% from P123 micelle-like particle. In 3 M [pmim][Br], there is negligible contribution of P123 micelle and ~90% of the DLS signal originates from a giant particle of diameter 3.5 μm (3500 nm). In this case, about 10 wt % of the aggregates remains as a big cluster of diameter 400 nm. This is also much larger than the free P123 micelle.

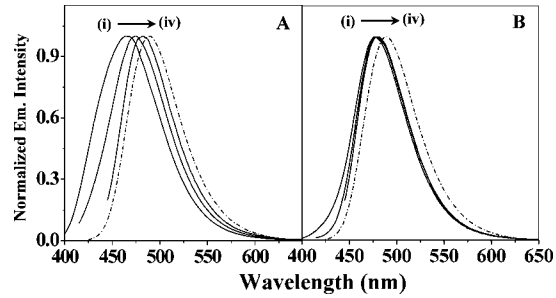

Figure 2. Emission spectra of C480 in 5 wt % P123 in water, λ_{ex} = (i) 375 nm, (ii) 405 nm, (iii) 435 nm, in (A) 0.9 M, (B) 3 M [pmim][Br], and (iv) in 0 wt % P123 (...) (λ_{ex} = 375−435 nm).

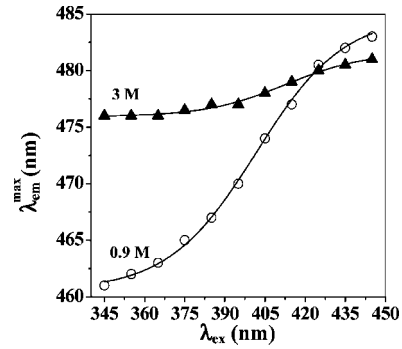

Figure 3. Plot of emission maximum of C480 in 5 wt % P123 as a function of λ_{ex} in 0.9 M (○) and 3 M [pmim][Br] (▲).

TABLE 2: λ_{ex} Dependence of the Steady State Emission Maximum of C480 in 5 wt % P123 in the Presence of [pmim][Br]

	λ_{em}^{max} (nm)			
	[pmim][Br]			
λ_{ex} (nm)	0 M	0.9 M	3 M	water
375	455	465	477	489
405	465	474	478	489
435	475	482	480	489

In summary, P123 and [pmim][Br] form a giant micron-sized cluster in an aqueous solution that are much bigger than the P123 micelles (~18 nm) or the [pmim][Br] particles (1.3 nm). Following Zheng et al.,[13a] we propose a structure of the P123-RTIL cluster with large scale penetration of the P123 micelle by the undissociated ion pair of the RTIL (Scheme 1D). In the following section, we investigate the giant P123-[pmim][Br] clusters using steady state spectroscopy, anisotropy decay, and solvation dynamics.

3.2. Steady State Absorption and Emission Spectra: λ_{ex} Dependence. The absorption and emission maxima of C480 display a prominent red shift with increase in polarity.[14] In bulk water, the emission maximum (λ_{em}^{max}) of C480 is at 489 nm. λ_{em}^{max} of C480 in an aqueous solution of 3 M [pmim][Br] is found to be at 480 nm which is blue shifted from that in water. This suggests a decrease in the local polarity around C480 in 3 M RTIL presumably because of clustering of the RTIL around the probe C480. Both in bulk water and in 3 M [pmim][Br], the emission maximum of C480 is independent of the excitation

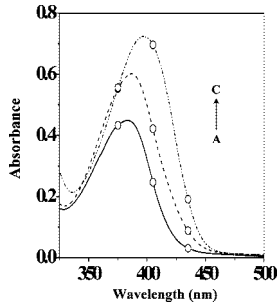

Figure 4. Absorption spectra of C480 in 5 wt % P123 (—) in (A) 0 M, (B) 0.9 M (----), and (C) 3 M [pmim][Br] (-•••-). The excitation wavelength are marked (○) at 375, 405, and 435 nm.

TABLE 3: Anisotropy Decay of C480 in Water (λ_{ex} = 405 nm) in the Presence of 0.9 and 3 M [pmim][Br] (without P123)

[pmim][Br] (mol/L)	r_0	τ^a_{rot} (ps)
0.9	0.30	200
3	0.27	400

[a] ±25 ps (in a picosecond setup).

wavelength (λ_{ex}). This suggests that the microenvironment of C480 in water and in 3 M RTIL is homogeneous.

λ^{max}_{em} of C480 exhibits a marked λ_{ex} dependence in a P123-RTIL aggregate. This is indicative of a highly heterogeneous microenvironment in the P123-RTIL aggregate. In 5 wt % P123 micelle and 0.9 M [pmim][Br], λ^{max}_{em} of C480 shifts from 461 nm for λ_{ex} = 345 to 483 nm at λ_{ex} = 445 nm (Figures 2A, 3 and Table 2). The 22 nm REES in the P123-RTIL aggregate is slightly smaller than the 25 nm REES reported earlier for a P123 micelle.[16e] As discussed in the case of P123 micelle,[16e] at a short λ_{ex} (345 nm), the C480 molecules in the hydrophobic PPO core region are excited while a long λ_{ex} (445 nm, red end) selects the C480 molecule in the hydrophilic PEO corona region. It may be noted that the λ^{max}_{em} of C480 in the P123-RTIL aggregate is red shifted relative to that in the P123 micelle. For instance at λ_{ex} = 345 nm, the λ^{max}_{em} in the P123-RTIL aggregate is red shifted by ~8 nm from that (453 nm) in a P123 micelle. Since excitation at 345 nm selects the C480 molecules in the core of P123 micelle, the ~8 nm red shift in 0.9 M RTIL indicates an increase in the local polarity of the core. The increase in the local polarity of P123 micelle on addition of RTIL may be ascribed to the penetration of the hydrophobic PPO core by the RTIL that is likely to stay as an undissociated ion pair inside the micelle. In the case of the corona region (λ_{ex} =445 nm), the λ^{max}_{em} in a P123-RTIL aggregate is 5 nm red shifted compared to that in P123 micelle.

In 3 M ([pmim][Br]), when the micron-sized P123-[pmim-][Br] aggregate are formed, the REES of C480 becomes very small (~5 nm, Figures 2B, 3 and Table 2). In this case, λ^{max}_{em} shifts from 476 nm at λ_{ex} = 345 to 481 nm at λ_{ex} = 445 nm. The smaller value of REES (5 nm) is in sharp contrast to the large REES in P123 micelle (25 nm) or that in a P123-[pmim][Br] (22 nm at 0.9 M RTIL). This suggests that in the micron-sized aggregate the polarity difference between the core and the corona is substantially lower. It may be noted that in 3 M [pmim][Br] and 5 wt % (8.7 mM) P123, there are ~340 RTIL molecules for every P123 molecule. Thus in the aggregate, RTIL vastly outnumbers P123. At such a high concentration, the RTIL invades both the core and corona region of the P123 micelle. This increases the polarity of the core and reduces the polarity difference between the core and the corona. λ^{max}_{em} of

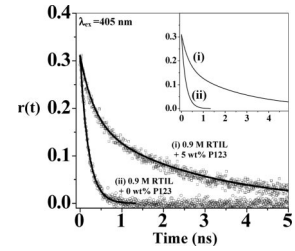

Figure 5. Fluorescence anisotropy decay of C480 in 0.9 M [pmim][Br] in water (i) 5 wt % P123 and (ii) 0 wt % P123, λ_{ex} =405 nm, λ_{em} =460 nm. Fitted curves of the decays are shown in the inset.

TABLE 4: Anisotropy Decay Parameters of C480 in 5 wt % P123 in the Absence and Presence of [pmim][Br] at Different Excitation Wavelengths

concentration of [pmim][Br] (mol/L)	λ_{ex} (nm)	r_0	decay parameters of $r(t)$ $\tau_{fast}{}^a$ (ps) (a_{fast})	$\tau_{slow}{}^a$ (ps) (a_{slow})	$\langle\tau_{rot}\rangle^b$ (ps)
0	375	0.36	650 (0.30)	3750 (0.70)	2800
	405	0.34	650 (0.25)	3750 (0.75)	3000
	435	0.33	350 (0.40)	2000 (0.60)	1350
0.9[c]	375	0.27	370 (0.35)	2800 (0.65)	1950
	405	0.31	320 (0.45)	2200 (0.55)	1350
	435	0.28	300 (0.80)	1000 (0.20)	450
3	375	0.35	350 (0.65)	1000 (0.35)	600
	405	0.27	350 (0.70)	1000 (0.30)	600
	435	0.32	350 (0.65)	1000 (0.35)	600

[a] ±25 ps (in a picosecond setup). [b] $\langle\tau_{rot}\rangle = a_{fast}\tau_{fast} + a_{slow}\tau_{slow}$. [c] For 0.9 M RTIL, the contribution of ~30% probe in P123 micelle is subtracted.

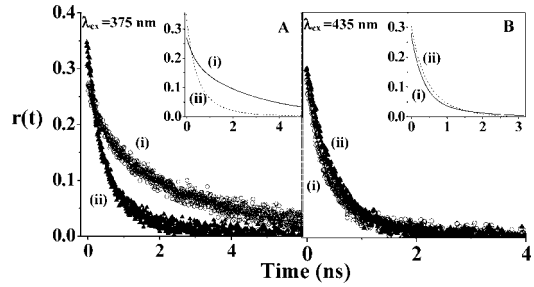

Figure 6. Fluorescence anisotropy decay of C480 in 5 wt % P123 at (A) λ_{ex} = 375 nm, λ_{em} = 460 nm and (B) λ_{ex} = 435 nm, λ_{em} = 460 nm in (i) 0.9 M and (ii) 3 M [pmim][Br]. Fitted curves of the decays are shown in the inset.

C480 in a P123-[pmim][Br] mixed micelle (481 nm) is very slightly red shifted from that in a 3 M aqueous solution of [pmim][Br].

The absorption maximum of C480 in P123 micelle (383 nm, Figure 4) is intermediate between those in acetonitrile (380 nm) and those in ethanol (387 nm) and is blue shifted by 13 nm from the absorption maximum (396 nm) in water.[14] Penetration of a P123 micelle by the ionic liquid, [pmim][Br] causes a red shift in the absorption maximum of C480 because of the increase in local polarity. On addition of 0.9 M [pmim][Br], the absorption maximum of C480 undergoes a red shift (Figure 4) to 387 nm which is identical to that in ethanol.[14] Further addition of [pmim][Br] to the P123 micelle causes a red shift of the absorption maximum of C480 to 396 nm at 3 M RTIL. This is same as the absorption maximum of C480 in water.

3.3. Fluorescence Anisotropy Decay of C480. The time constant of fluorescence anisotropy decay of C480 in bulk water is 70 ps.[20] The time constant of anisotropy decay of C480 in an aqueous solution of [pmim][Br] is found to be slightly longer,

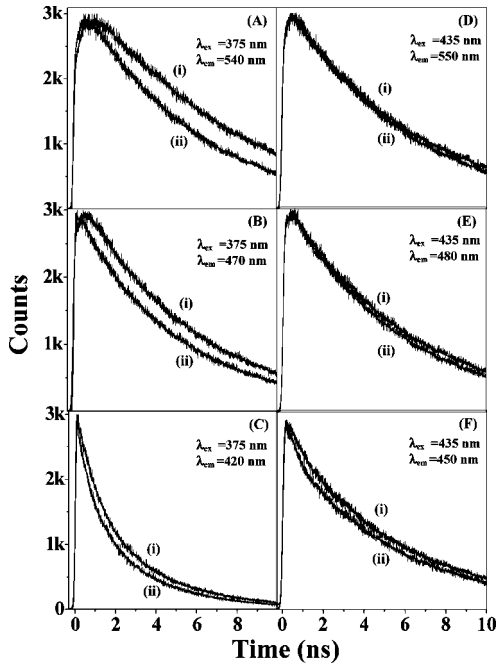

Figure 7. Picosecond decays of C480 in 5 wt % P123, in the presence of (i) 0.9 M and (ii) 3 M [pmim][Br].

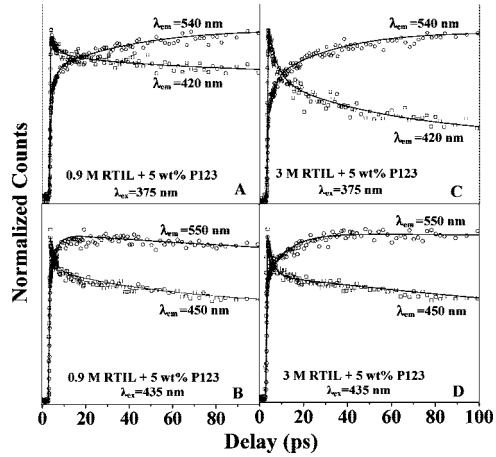

Figure 8. Femtosecond transients of C480 in P123-[pmim][Br] mixed micelle.

single exponential and independent of λ_{ex}. The time constant of the anisotropy decay is found to be 200 ps in 0.9 M RTIL and 400 ps in 3 M RTIL (Table 3). The slightly longer rotational time suggests increased friction in the microenvironment of C480 on addition of RTIL. The lack of λ_{ex} dependence of the anisotropy decay suggests that the microscopic friction sensed by C480 in an aqueous solution of [pmim][Br], is quite uniform. Since the particle size in an aqueous solution of 3 M RTIL (1.3 nm from DLS study) is close to the diameter of C480 the uniform environment is quite expected.

The fluorescence anisotropy decay of C480 in P123 micelle and P123-RTIL exhibits two major differences from that in an aqueous solution of RTIL. First, the decay is biexponential with one very long component (2800 ps in 0.9 M RTIL and 1000 ps in 3 M RTIL). Figure 5 shows the difference in the anisotropy decay of C480 in a 0.9 M aqueous solution of RTIL in the absence and in the presence of 5 wt % P123. The average rotational time in 5 wt % P123 (1350 ps) is about 7 times longer than the rotational time (200 ps) in the absence of P123.

The second important difference in the anisotropy decay in the presence of P123 is the marked λ_{ex} dependence particularly

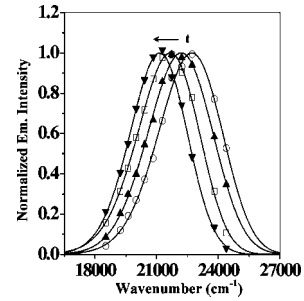

Figure 9. Time resolved emission spectra (TRES) of C480 (λ_{ex}=375 nm) in 5 wt % P123 in 0.9 M [pmim] [Br] at 0 ps (○), 350 ps (▲), 3500 ps (□) and 12 000 ps (▼).

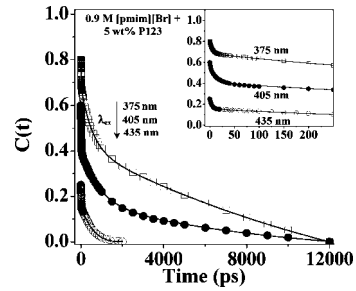

Figure 10. Decay of solvent response function $C(t)$ of C480 in 5 wt % P123 in 0.9 M [pmim][Br], λ_{ex} at 375 nm (□), 405 nm (●) and 435 nm (○). The points denote the actual values of $C(t)$ and the solid line denotes the best fit. Initial portions of the decays are shown in the inset.

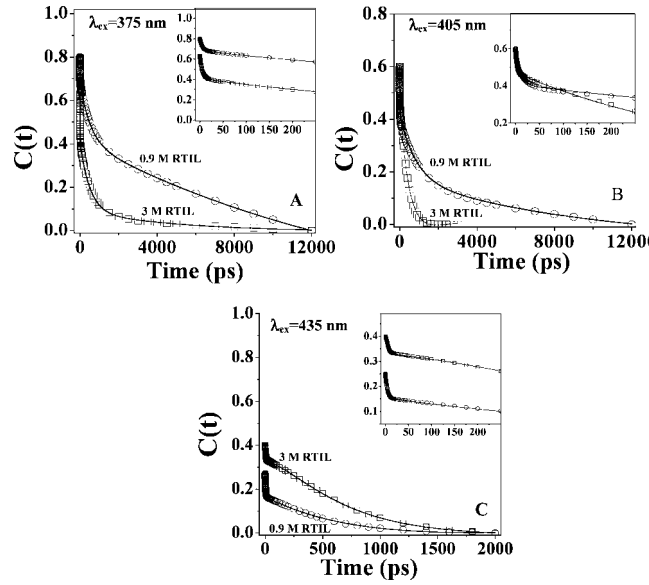

Figure 11. Decay of solvent response function $C(t)$ of C480 in 5 wt % P123 for (A) λ_{ex} = 375 nm, (B) λ_{ex} = 405 nm and (C) λ_{ex} = 435 nm in 0.9 M (○) and 3 M [pmim][Br] (□). The points denote the actual values of $C(t)$ and the solid line denotes the best fit. Initial portions of the decays are shown in the inset.

in 0.9 M RTIL. For a mixed micelle containing 0.9 M [pmim][Br] and 5 wt % P123, 30% of the signal arises from P123 micelle like particle.[17d] This contribution was subtracted from both $I_{||}$ and $I_{\perp}$. When this correction is done, $<\tau_{rot}>$ of C480 in the core (λ_{ex} = 375 nm) is found to be 1950 ps and that at the corona is ~450 ps for λ_{ex}=435 nm (Table 4, Figure 6). Similar λ_{ex} dependence of anisotropy decay is earlier reported in a P123 micelle with $<\tau_{rot}>$ = 2800 ps in the core and 1350 ps in the corona region.[17d] Evidently, addition of 0.9 M RTIL to the P123 micelle decreases $<\tau_{rot}>$ both at the core and the

TABLE 5: Decay Parameters of $C(t)$ of C480 in 5 wt % P123 Micelle in the Presence of 0.9 and 3 M [pmim][Br] at Different Excitation Wavelength (λ_{ex})

	$\Delta\nu_{obs}$[a] ($\nu(0)$) (cm^{-1})		decay parameter of $C(t)$, τ_i[b] (a_i) (ps)			
			0.9 M [pmim][Br][d]		3 M [pmim][Br]	
λ_{ex}(nm)	0.9 M RTIL	3 M RTIL		$<\tau_s>$		$<\tau_s>$
375	1400 (22360)	850 (21640)	<0.3 (20%)[c], 4 (15%) 500 (20%), 4000 (45%)	1900	<0.3 (35%),[c] 4 (20%), 500(35%), 4000 (10%)	500
405	1320 (21890)	800 (21600)	<0.3 (40%)[c], 4 (20%) 500 (20%), 4000 (20%)	900	<0.3 (40%)[c], 4 (15%), 500 (45%)	250
435	570 (21090)	525 (21350)	<0.3 (75%)[c] 4 (10%), 500 (15%)	75	<0.3 (60%)[c], 4 (5%), 500 (35%)	175

[a] ± 100 cm^{-1}. [b] $\pm 10\%$. [c] Calculated using Fee−Maroncelli Method.[19b] [d] For 0.9 M RTIL, the contribution of ~30% probe in P123 micelle is subtracted.

TABLE 6: Decay Parameters of $C(t)$ of C480 in Water in the Presence of 0.9 and 3 M [pmim][Br] at Excitation Wavelength (λ_{ex}) 405 nm

[pmim][Br]	$\Delta\nu_{obs}$[a] ($\nu(0)$) (in cm^{-1})	decay parameters of $C(t)$, τ_i[b] (a_i) (ps)	$<\tau_s>$ (ps)
0.9 M	475 (21050)	<0.3 (70%),[c] 4 (5%), 500 (25%)	130
3 M	725 (21500)	<0.3 (45%),[c] 4 (15%), 500 (40%)	200

[a] ± 100 cm^{-1}. [b] $\pm 10\%$. [c] Calculated using Fee−Maroncelli Method.[19b]

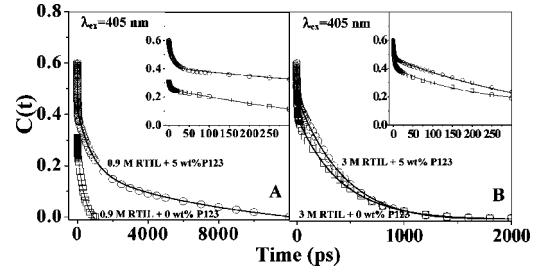

Figure 12. Decay of solvent response function $C(t)$ of C480 in 5 wt % P123 (○) and 0 wt % P123 (□) for (A) 0.9 M and (B) 3 M [pmim][Br] at $\lambda_{ex} = 405$ nm. The points denote the actual values of $C(t)$ and the solid line denotes the best fit. Initial portions of the decays are shown in the inset.

corona. The faster anisotropy decay suggests disentanglement of the P123 chains by penetration of RTIL.

In 3 M [pmim][Br], the average rotational relaxation time of C480 in P123-[pmim][Br], shows hardly any λ_{ex} dependence (Figure 6). In this case, the average rotational relaxation time is 600 ps both at $\lambda_{ex} = 375$ nm and at $\lambda_{ex} = 435$ nm. Thus in 3 M ionic liquid, the microscopic friction in the core and the corona of the P123-[pmim][Br] giant aggregate are almost identical. However, the rotational time in this case is longer than that (400 ps) in a 3 M aqueous solution of the RTIL.

3.4. Solvation Dynamics of C480 in P123-[pmim][Br] Aggregate. Finally, we investigated the solvation dynamics in different regions of the P123-[pmim][Br] aggregate through variation of λ_{ex}. Figures 7 and 8 show the picosecond and femtosecond transients of C480 in P123 micelle in the presence of 0.9 and 3 M [pmim][Br]. Figure 9 shows the time-resolved emission spectra (TRES) of C480 in a P123-[pmim][Br] mixed micelle for $\lambda_{ex} = 375$ nm.

At all λ_{ex}, the emission decays of C480 in a P123 micelle in the presence of 0.9 and 3 M ionic liquid display marked wavelength dependence with a rise at the red end and decay at the blue end. This is a clear indication of solvation dynamics. Figures 10 and 11 show the decays of solvent response function, $C(t)$ for different excitation wavelengths and Table 5 summarizes the decay parameters of $C(t)$ along with dynamic solvent shift (DSS).

For the mixed micelle containing 0.9 M [pmim][Br] and 5 wt % P123, contribution of 30% micelle-like particle is subtracted from each of the TRES. This gives exclusively contribution of the 40 nm sized particle. In this case, the total dynamic Stokes shift, (DSS = $\nu(0) - \nu(\infty)$), decreases 2.5 times from 1400 to 570 cm^{-1} with increase in λ_{ex} from 375 to 435 nm (Table 5). This is accompanied by a nearly 25 times decrease in the average solvation time ($<\tau_s>$) from 1900 to 75 ps (Table 5). For $\lambda_{ex} = 375$ nm (i.e., for the core) almost the entire amount of solvation is captured. The decrease in DSS and average solvation time with increase in λ_{ex} implies that the solvation dynamics is faster in the corona region (probed at $\lambda_{ex} = 435$ nm) than that in the core (selected at $\lambda_{ex} = 375$ nm).

For the micron-sized aggregate (3 M [pmim][Br] and 5 wt % P123, diameter 3500 nm), the solvation dynamics is found be faster than that in the 40 nm particle. The λ_{ex} dependence of solvation dynamics in the micron-sized particle is less prominent than that in the 40 nm particle (0.9 M RTIL). For the micron-sized particle, the DSS decreases ~1.5 times from 850 cm^{-1} at $\lambda_{ex} = 375$ nm to 525 cm^{-1} at $\lambda_{ex} = 435$ nm while the average solvation time decreases about 3 times from 500 to 175 ps (Table 5). It is interesting to note that the λ_{ex} variation of solvation dynamics is significant in the micron-sized particle, even though there is very little λ_{ex} dependence of λ_{em}^{max} (REES) and anisotropy decay. This further demonstrates that solvation dynamics is more sensitive to the regions (i.e., λ_{ex} variation) than the steady state λ_{em}^{max} and anisotropy decay.

The different magnitude of λ_{ex} variation of the 3500 and the 40 nm particle may be ascribed to their structures. In the 40 nm particle (RTIL/P123 molar ratio ~100) the difference in the core and corona region are quite large and the ultraslow core is still retained. In the micron-sized particle (RTIL/P123 molar ratio ~340), the core is affected to a very large extent and the contribution of ultraslow component (~4000 ps) arising from the core is very small. Thus the average solvation time is very short in the micron-sized particle.

3.5. Solvation Dynamics of C480 in an Aqueous Solution of [pmim][Br] in the Absence of P123. The solvation time for C480 in an aqueous solution of [pmim][Br] is found to be 130 ps for 0.9 M RTIL and 200 ps for 3 M RTIL in water (Table 6 and Figure 12). In this case, there is no λ_{ex} dependence of solvation dynamics. It is evident that the solvation dynamics in the aqueous solution of the RTIL is much faster than that in the core region ($\lambda_{ex} = 375$ nm) in P123-RTIL aggregate with 0.9 M [pmim][Br] (1900 ps) and in 3 M [pmim][Br] (500 ps) but is comparable to the exposed corona region of the P123-RTIL aggregate.

The solvation dynamics observed in an aqueous solution of the RTIL is much slower than that in bulk water (~1 ps). The

slower dynamics is consistent with previous experimental and theoretical studies on slow solvation dynamics in a binary mixture[21] and in an aqueous solution of an ionic liquid.[22]

4. Conclusion

This work demonstrates that the RTIL, [pmim][Br], affects the structure and dynamics of the P123 micelle. The P123-[pmim][Br] aggregate (40 nm in 0.9 M RTIL and 3500 nm in 3 M RTIL) is much bigger than the P123 micelle (18 nm). The anisotropy decay and solvation dynamics in a P123-RTIL mixed micelle (at 0.9 M) is faster than those in P123 micelle. This and the red shift of emission maxima suggest penetration of P123 micelle by RTIL ion pairs. Dynamics in different regions in the P123-[pmim][Br] mixed micelle are studied by varying the λ_{ex}. In 0.9 M [pmim][Br] and P123, the anisotropy decays and solvation dynamics of C480 at the corona region (λ_{ex} = 435 nm) are respectively, 4 and 25 times faster than those in the core (λ_{ex} = 375 nm). This suggests that in the presence of 0.9 M RTIL there is large difference in the core and corona region. In the giant (3500 nm) cluster (3 M RTIL and 5 wt % P123), large scale invasion of the P123 micelle by the RTIL ion-pairs somewhat blurs the difference between the core and corona. In this case, anisotropy decay at the core and corona are similar (~600 ps). However, solvation dynamics in the corona is still ~3 times faster than that in the core region. The dynamics (anisotropy decay and solvation dynamics) in the P123-RTIL aggregate are found to be quite different from that in an aqueous solution of the RTIL.

Acknowledgment. Thanks are due to Department of Science and Technology, India (Project Number IR/I1/CF-01/2002 and J. C. Bose Fellowship) and Council for Scientific and Industrial Research (CSIR) for generous research support. S.D., A.A., D.K.D., and D.K.S. thank CSIR for awarding fellowships.

References and Notes

(1) (a) Wang, Y.; Jiang, W.; Yan, T.; Voth, G. A. *Acc. Chem. Res.* **2007**, *40*, 1193. (b) Castner, E. W., Jr.; Wishart, J. F.; Shirota, H. *Acc. Chem. Res.* **2007**, *40*, 1217. (c) Iwata, K.; Okajima, H.; Saha, S.; Hamaguchi, H. *Acc. Chem. Res.* **2007**, *40*, 1174. (d) Samanta, A. *J. Phys. Chem. B* **2006**, *110*, 13704. (e) Lei, Z.; Chen, B.; Li, C.; Liu, H. *Chem. Rev.* **2008**, *108*, 1419. (f) Haumann, M.; Riisager, A. *Chem. Rev.* **2008**, *108*, 1474.

(2) (a) Hardacre, C.; Holbrey, J. D.; McMath, S. E. J.; Bowron, D. T.; Soper, A. K. *J. Chem. Phys.* **2003**, *118*, 273. (b) Li, J.; Wang, I.; Fruchey, K.; Fayer, M. D. *J. Phys. Chem. A* **2006**, *110*, 10384.

(3) (a) Pal, A.; Samanta, A. *J. Phys. Chem. B* **2007**, *111*, 4724. (b) Paul, A.; Mandal, P. K.; Samanta, A. *J. Phys. Chem. B* **2005**, *109*, 9148. (c) Karmakar, R.; Samanta, A. *J. Phys. Chem. A* **2002**, *106*, 6670. (d) Mandal, P. K.; Sarkar, M.; Samanta, A. *J. Phys. Chem. A* **2004**, *108*, 9048. (e) Karmakar, R.; Samanta, A. *J. Phys. Chem. A* **2002**, *106*, 4447. (f) Paul, A.; Samanta, A. *J. Phys. Chem. B* **2008**, *112*, 947.

(4) (a) Jin, H.; Baker, G. A.; Arzhantsev, S.; Dong, J.; Maroncelli, M. *J. Phys. Chem. B* **2007**, *111*, 7291. (b) Jin, H.; Li, X.; Maroncelli, M. *J. Phys. Chem. B* **2007**, *111*, 13473. (c) Ito, N.; Arzhantsev, S.; Maroncelli, M. *Chem. Phys. Lett.* **2004**, *396*, 83. (d) Arzhantsev, S.; Jin, H.; Baker, G. A.; Maroncelli, M. *J. Phys. Chem. B* **2007**, *111*, 4978. (e) Ito, N.; Arzhantsev, S.; Heitz, M.; Maroncelli, M. *J. Phys. Chem. B* **2004**, *108*, 5771.

(5) (a) Funston, A. M.; Fadeeva, T. A.; Wishart, J. F.; Castner, E. W., Jr *J. Phys. Chem. B* **2007**, *111*, 4963. (b) Shirota, H.; Castner, E. W., Jr *J. Phys. Chem. B* **2007**, *111*, 4819. (c) Shirota, H.; Funston, A. M.; Wishart, J. F.; Castner, E. W., Jr *J. Chem. Phys.* **2005**, *122*, 184512.

(6) (a) Annapureddy, H. V. R.; Hu, Z.; Xia, J.; Margulis, C. J. *J. Phys. Chem. B* **2008**, *112*, 1770. (b) Hu, Z.; Margulis, C. J. *Proc. Natl. Acad. Sci. U.S.A.* **2006**, *103*, 831. (c) Kobrak, M. N. *J. Chem. Phys.* **2007**, *127*, 184507. (d) Jeong, D.; Shim, Y.; Choi, M. Y.; Kim, H. J. *J. Phys. Chem. B* **2007**, *111*, 4920. (e) Liu, X.; Zhou, G.; Zhang, S.; Wu, G.; Yu, G. *J. Phys. Chem. B* **2007**, *111*, 5658.

(7) (a) Wang, Y.; Voth, G. A. *J. Am. Chem. Soc.* **2005**, *127*, 12192. (b) Bhargava, B. L.; Devane, R.; Klein, M. L.; Balasubramanium, S. *Soft Matter* **2007**, *3*, 1395. (c) Bhargava, B. L.; Balasubramanian, S. *J. Chem. Phys.* **2006**, *125*, 219901. (d) Lopes, J. N. A. C.; Padua, A. A. H. *J. Phys. Chem. B* **2006**, *110*, 3330.

(8) (a) Triolo, A.; Russina, O.; Bleif, H.-J.; Di Cola, E. *J. Phys. Chem. B* **2007**, *111*, 4641. (b) Xiao, D.; Rajian, J. R.; Cady, A.; Li, S.; Bartsch, R. A.; Quitevis, E. L. *J. Phys. Chem. B* **2007**, *111*, 4669.

(9) (a) Shigeto, S.; Hamaguchi, H. *Chem. Phys. Lett.* **2006**, *427*, 329. (b) Katayanagi, H.; Hayashi, S.; Hamaguchi, H.; Nishikawa, K. *Chem. Phys. Lett.* **2004**, *392*, 460.

(10) (a) Adhikari, A.; Sahu, K.; Dey, S.; Ghosh, S.; Mandal, U.; Bhattacharyya, K. *J. Phys. Chem. B* **2007**, *111*, 12809. (b) Adhikari, A.; Dey, S.; Das, D. K.; Mandal, U.; Ghosh, S.; Bhattacharyya, K. *J. Phys. Chem. B* **2008**, *112*, 6350.

(11) (a) Goldmints, I.; von Gottberg, K.; Smith, K. A.; Hatton, T. A. *Langmuir* **1997**, *13*, 3659. (b) Mortensen, K. *Macromolecules* **1997**, *30*, 503. (c) Hecht, E.; Mortensen, K.; Gradzielski, M.; Hoffmann, H. *J. Phys. Chem.* **1995**, *99*, 4866. (d) Wanka, G.; Hoffmann, H.; Ulbricht, W. *Macromolecules* **1994**, *27*, 4145. (e) Ganguly, R.; Aswal, V. K.; Hassan, P. A.; Gopalakrishnan, I. K.; Kulshreshtha, S. K. *J. Phys. Chem. B* **2006**, *110*, 9843.

(12) Shimizu, S; McLaren, W. M.; Matubayasi, N. *J. Chem. Phys.* **2006**, *124*, 234905.

(13) (a) Zheng, L.; Guo, C.; Wang, J.; Liang, X.; Chen, S.; Ma, J.; Yang, B.; Jiang, Y.; Liu, H. *J. Phys. Chem. B* **2007**, *111*, 1327. (b) Seddon, K. R.; Stark, A.; Torres, M. J. *Pure Appl. Chem.* **2000**, *72*, 2275. (c) Behera, K.; Pandey, S. *J. Phys. Chem. B* **2007**, *111*, 13307. (d) Behera, K.; Pandey, M. D.; Porel, M.; Pandey, S. *J. Chem. Phys.* **2007**, *127*, 184501.

(14) Jones, G., II; Jackson, W. R.; Choi, C.-Y.; Bergmark, W. R. *J. Phys. Chem.* **1985**, *89*, 294.

(15) (a) Demchenko, A. P. *Luminescence* **2002**, *17*, 19. (b) Demchenko, A. P. *Biophys. Chem.* **1982**, *15*, 101. (c) Lakowicz, J. R. *Biochemistry* **1984**, *23*, 3013. (d) Mukherjee, S.; Chattopadhyay, A. *Langmuir* **2005**, *21*, 287. (e) Kelkar, D. A.; Chattopadhyay, A. *J. Phys. Chem. B* **2004**, *108*, 12151.

(16) (a) Humpolickova, J.; Stepanek, M.; Prochazka, K.; Hof, M. *J. Phys. Chem. A* **2005**, *109*, 10803. (b) Grant, C. D.; Steege, K. E.; Bunagan, M. R.; Castner, E. W., Jr *J. Phys. Chem. B* **2005**, *109*, 22273. (c) Grant, C. D.; DeRitter, M. R.; Steege, K. E.; Fadeeva, T. A.; Castner, E. W., Jr *Langmuir* **2005**, *21*, 1745. (d) Mali, K. S.; Dutt, G. B.; Mukherjee, T. *J. Chem. Phys.* **2006**, *124*, 054904. (e) Sen, P.; Ghosh, S.; Sahu, K.; Mondal, S. K.; Bhattacharyya, K. *J. Chem. Phys.* **2006**, *124*, 204905.

(17) (a) Satoh, T.; Okuno, H.; Tominaga, K.; Bhattacharyya, K. *Chem. Lett.* **2004**, *33*, 1090. (b) Sen, P.; Satoh, T.; Bhattacharyya, K.; Tominaga, K. *Chem. Phys. Lett.* **2005**, *411*, 339. (c) Mandal, U.; Ghosh, S.; Mitra, G.; Adhikari, A.; Dey, S.; Bhattacharyya, K. *Chem. Asian J.* **2008**, *3*, 1430. (d) Mandal, U.; Adhikari, A.; Dey, S.; Ghosh, S.; Mondal, S. K.; Bhattacharyya, K. *J. Phys. Chem. B* **2007**, *111*, 5896. (e) Ghosh, S.; Adhikari, A.; Mandal, U.; Dey, S.; Bhattacharyya, K. *J. Phys. Chem. C* **2007**, *111*, 8775. (f) Adhikari, A.; Dey, S.; Mandal, U.; Das, D. K.; Ghosh, S.; Bhattacharyya, K. *J. Phys. Chem. B* **2008**, *112*, 3575.

(18) Namboodiri, V. V.; Varma, R. S. *Org. Lett.* **2002**, *4* (18), 3161.

(19) (a) Maroncelli, M.; Fleming, G. R. *J. Chem. Phys.* **1987**, *86*, 6221. (b) Fee, R. S.; Maroncelli, M. *Chem. Phys.* **1994**, *183*, 235.

(20) (a) Shirota, H.; Segawa, H. *J. Phys. Chem. A* **2003**, *107*, 3719. (b) Shirota, H. *J. Phys. Chem. B* **2005**, *109*, 7053.

(21) (a) Chicos, F.; Willert, A.; Rempel, U.; von Borczyskowski, C. *J. Phys. Chem. A* **1997**, *101*, 8179. (b) Luther, B. M.; Kimmel, J. R.; Levinger, N. E. *J. Chem. Phys.* **2002**, *116*, 3370. (c) Ladanyi, B. M.; Perng, B. C. *J. Phys. Chem. A* **2002**, *106*, 6922. (d) Molotsky, T.; Huppert, D. *J. Phys. Chem. A* **2003**, *107*, 8449. (e) Mukherjee, S.; Sahu, K.; Roy, D.; Mondal, S. K.; Bhattacharyya, K. *Chem. Phys. Lett.* **2004**, *384*, 128.

(22) (a) Chakrabarty, D.; Chakrabarty, A.; Seth, D.; Hazra, P.; Sarkar, N. *Chem. Phys. Lett.* **2004**, *397*, 469. (b) Chakrabarty, D.; Chakrabarty, A.; Seth, D.; Sarkar, N. *J. Phys. Chem. A* **2005**, *109*, 1764.

JP804401P